Published in final edited form as:

J Neuropsychiatry Clin Neurosci. 2019 ; 31(4): 368–377. doi:10.1176/appi.neuropsych.18060131.

Working Memory is Associated with Distributed Executive Control Networks in Schizophrenia

Korey P. Wylie, M.D.[a,*], **Josette G. Harris, Ph.D.**[a], **Debashis Ghosh, Ph.D.**[b], **Ann Olincy, M.D.**[a], **Jason R. Tregellas, Ph.D.**[a,c]

[a]Department of Psychiatry, University of Colorado Anschutz Medical Campus, Bldg. 500, Mail Stop F546, 13001 East 17th Place, Aurora, CO, 80045, USA

[b]Department of Biostatistics and Informatics, Colorado School of Public Health, Mail Stop B119, 13001 East 17th Place, Aurora, CO, 80045, USA

[c]Research Service, Denver VA Medical Center, Research Service (151), Eastern Colorado Health System, 1055 Clermont St., Denver, CO, 80220, USA

Abstract

Working memory impairments represent a core cognitive deficit in schizophrenia, predictive of patients' daily functioning, and one that is unaffected by current treatments. To address this, working memory is included in the MATRICS Consensus Cognitive Battery (MCCB), a standardized cognitive battery designed to facilitate drug development targeting cognitive symptoms. The neurobiology underlying these deficits in MCCB working memory is currently unknown, however, mirroring the poor understanding of working memory deficits in general in schizophrenia. To investigate this neurobiology, 28 subjects with schizophrenia were administered working memory tests from the MATRICS Consensus Cognitive Battery (MCCB) and examined with resting state fMRI. Intrinsic Connectivity Networks were estimated with Independent Components Analysis. Every voxel's time series was correlated with each network time series, creating a feature vector for voxel-level connectivity analysis. This feature vector was associated with working memory using the Distance Covariance statistic. Results demonstrated that the neurobiology of MCCB working memory tests largely follows the multi-component model of working memory, but revealed unexpected differences. The dorsolateral prefrontal cortex was not associated with working memory. The Central Executive system was instead associated with delocalized Right and Left Executive Control Networks. The Phonologic Loop within the multicomponent model, a subsystem involved in storing linguistic information, was associated with connectivity to the left temporoparietal junction and inferior frontal gyrus. However, connections to the Language Network did not predict working memory test performance. These results provide supporting evidence for the multi-component model of working memory in terms of the biology underlying the MCCB.

[*]Corresponding author: Korey P. Wylie, Anschutz Medical Campus Bldg. 500, Mail Stop F546, 13001 East 17th Place, Aurora, CO, 80045, telephone: 303-724-5537, Fax: 303-724-4956, Korey.Wylie@ucdenver.edu.

Conflicts of Interest

The authors report no financial relationships with commercial interests.

Keywords

Working Memory; Multi-component Model; MATRICS Consensus Cognitive Battery; Functional Connectivity; Independent Components Analysis; Distance Covariance

Introduction

Individuals with schizophrenia suffer from symptoms that include intrusive thoughts and sensory stimuli, psychosocial deficits in emotional expression, and cognitive deficits, generally referred to as positive, negative, and cognitive symptoms, respectively. While antipsychotic medications successfully control symptoms related to intrusive sensory stimuli such as hallucinations, they are not able to treat the emotional and cognitive symptoms of schizophrenia. These medication's success in controlling the overt symptoms of psychosis, yet often failing to restore patients to their level of functioning prior to the onset of illness, thus highlights the suffering caused by other core symptoms of schizophrenia. For instance, from the patient's perspective, medical treatments that only control hallucinations are of limited value if other, untreated symptoms prevent them from socializing and pursuing life and career goals. These other core symptoms include untreated, and currently untreatable, cognitive deficits.

Impaired working memory is a core cognitive deficit in schizophrenia. Problems in working memory, defined as the temporary storage and manipulation of information, are common in patients with the disease {1,2}. They predate the onset of psychotic symptoms and may underlie deficits in other cognitive domains {3, 4}. Most importantly, they are strongly predictive of impairments in social and vocational outcomes such as employment status, educational achievement, and independent living {5, 6}. Specifically, in adults with schizophrenia, working memory test performance predicts work or education functioning {6}. In adolescents with schizophrenia, baseline working memory performance is significantly related to social, communication, personal and community living skills at a follow-up visit one year later {5}. No current treatment is able to ameliorate the suffering caused by this core cognitive deficit {7}. Consequently, working memory is included as a domain in the MATRICS Consensus Cognitive Battery (MCCB). The MCCB is a comprehensive battery of cognitive tests, designed for and extensively validated in subjects with schizophrenia, in order to facilitate drug development targeting cognitive symptoms {8}. While the neurobiology of many cognitive domains in the MCCB is currently unknown, the functional neuroanatomy of working memory in other contexts has been studied in detail in the field of cognitive neuroscience {9}. However, how the neurobiology of the specific tests in the MCCB, and how this neurobiology relates to other tests of working memory such as the n-back or item recognition tests, is currently unknown.

The neurobiology of working memory is associated with prefrontal brain regions, including the dorsolateral prefrontal cortex (dlPFC), the ventrolateral prefrontal cortex (vlPFC) encompassing the inferior frontal gyrus (IFG), as well as posterior parietal regions, including the intraparietal sulcus (IPS) and temporoparietal junction (TPJ) {10, 11}. Within the prefrontal cortices, the primary locus of activity differs by task. The dlPFC seems more

involved during complex cognitive tasks, including the n-back, in which subjects monitor a series of stimuli while deciding if the currently displayed item matches the stimulus presented n stimuli previously {12}. In contrast, the vlPFC is more involved during tasks involving simpler mental manipulations, such as the Sternberg Item Recognition Paradigm, in which subjects memorize a set of stimuli and, following a short delay, determine if a probe stimuli was included in this memorized set {10, 11}. The n-back is cognitively demanding, requiring continual updating of contents stored in memory. In contrast, item recognition tasks typically involve mental manipulations of static items in stored in memory, with lower processing demands. These different processing demands may account for the differences in the neurobiological responses to each task.

Similarly, the neurobiology of working memory deficits in schizophrenia also differs depending on the specific task, with both increased or decreased prefrontal response observed during different tasks. For example, compared to healthy controls, the n-back test elicits decreased dlPFC activity in patients with schizophrenia, while the Sternberg Item Recognition Paradigm elicits increased dlPFC activity {13, 14}. Similarly, the n-back test is associated with decreased vlPFC response in patients, including in the IFG, while the Sternberg Item Recognition Paradigm elicits increased IFG response {13, 15}.

In summary, the neurobiology of working memory deficits in schizophrenia depends on the nature of the specific test, with both increased and decreased prefrontal activity in response to different tasks. Given these seemingly contradictory results when comparing other working memory tests, the neurobiology that underlies the working memory deficit the MCCB is designed to measure is currently unknown, despite a wealth of information on working memory in general and in schizophrenia in particular. More sophisticated analytic methods are required to better understand the neurobiology of the MCCB.

The intrinsic network architecture within the brain may provide insight into the neurobiology of working memory as assessed by the MCCB. In the emerging consensus of whole-brain neural connectivity, the brain is divided into segregated functional processing systems, or Intrinsic Connectivity Networks (ICNs). These ICNs include networks dedicated to processing unimodal sensory information such as the Auditory Network, as well as networks dedicated to higher-level processing, including Left and Right Central Executive Networks (LECN and RECN, respectively) {16}. Interactions between ICNs occur at discrete anatomical locations within the brain, frequently referred to as processing hubs. This intrinsic functional architecture is stable across processing states or psychological tasks, forming a baseline organization of connectivity within the brain {17}. This fundamental network architecture facilitates specific task performance due to the efficient arrangement of its processing pathways {18}. Task-related activity induces minor rearrangements in the intrinsic network architecture based on processing demands {19}. Importantly, since this architecture is relatively constant during rest or active processing, investigations using resting state fMRI may be able to provide insights into the networks and regions where intrinsic network architecture predicts task performance.

This study investigates the neurobiology of MCCB-measured working memory deficits in schizophrenia by examining their relationship to intrinsic network architecture with resting

state fMRI and a novel network analysis technique, Distance Covariance {20}. This technique investigates multivariate associations between cognitive measures, neuroanatomy, and the delocalized processing systems that contribute to working memory. Results are interpreted using the framework provided by Baddeley's multicomponent model of working memory {21}.

The multicomponent model consists of separate storage buffers for different information types, the Visuospatial Sketchpad, the Episodic Buffer, and the Phonologic Loop, in combination with a Central Executive control system that acts on the information contained in the storage buffers (Figure 1). Each system corresponds to known functional neuroanatomy {21,22}. For example, verbal information is stored in language areas of the Phonologic Loop, such as Wernicke's and Broca's areas, located in the left TPJ and IFG respectively in most subjects. Similarly, the Central Executive is commonly localized to the bilateral dlPFC.

Recent investigations call into question the previously exclusive and one-to-one relationship between neuroanatomy and function in the multicomponent model. These studies suggest that the Central Executive system, in addition to the dlPFC, also includes the vlPFC as well as superior parietal regions such as the IPS {10, 23}. This suggests that the Central Executive system, rather than being localized to a single region, may instead be a distributed and delocalized processing system, which extends beyond neuroanatomical boundaries to encompass multiple regions. Other large-scale ICNs encompass entire neural processing systems and are active during cognitive states ranging from unfocused rest to most, if not all, deliberative cognitive tasks. In fact, two prominent ICNs, the RECN and LECN, encompass the prefrontal and parietal regions attributed to the delocalized Central Executive system. The study of these large-scale networks, along with their impact on cognitive processing, is a current topic of active investigation in resting state fMRI.

The current study examines MCCB working memory using resting state fMRI, focusing on delocalized networks and the connections included in the multi-component model (Figure 2). We will test connections between all ICNs and all voxels, in order to comprehensively examine how intrinsic network architecture contributes to working memory performance in schizophrenia.

We hypothesize that the multi-component model (Figure 1) will be reflected in the combined interactions of delocalized networks with anatomical regions (Figure 2). Specifically, we hypothesize that MCCB working memory in schizophrenia will be associated with connectivity to the left IFG, vlPFC, TPJ, and right IPS, and that the Central Executive system will be best represented by the right and left Executive Control Networks (RECN and LECN). These hypotheses are tested using a novel combination of multivariate statistical techniques.

Methods

Participants

Thirty-three subjects with schizophrenia or schizoaffective disorder were recruited via advertisements in the community and through outpatient clinics (Table 1). All patients met DSM-IV criteria for schizophrenia or schizoaffective disorder, confirmed by the Structured Clinical Interview for DSM-IV (SCID). Seven subjects were treated with typical antipsychotic medications, 23 with atypical antipsychotics, and two were unmedicated. All subjects were clinically stable outpatients, and were treated with the same antipsychotic regimen for at least three months. Five subjects were excluded due to excessive movement (>3 mm) during scanning. Exclusion criteria included a current diagnosis of substance abuse, neurological disorders, or head trauma, as well as MRI exclusion factors (claustrophobia, weight >300 lb, metal in the body). Only decision capable individuals were eligible for study participation. All subjects provided written informed consent after receiving a complete description of the study, and received compensation for their participation. The study was approved by the Colorado Multiple Institutional Review Board.

Cognitive Measures

The MCCB has been described in detail elsewhere {8}. Briefly, the battery consists of individual tests covering the cognitive domains of working memory (Wechsler Memory Scale-III, Spatial Span and Letter-Number Span subtests), speed of processing (Trail Making Test, part A; Brief Assessment of Cognition in Schizophrenia, symbol coding subtest; and category fluency test), attention and vigilance (Continuous Performance Test-Identical Pairs Version), verbal learning (Hopkins Verbal Learning Test-Revised), visual learning (Brief Visuospatial Memory Test–Revised), reasoning and problem solving (Neuropsychological Assessment Battery, mazes subtest), and social cognition (Mayer-Salovey-Caruso Emotional Intelligence Test, managing emotions subtest). Raw scores were converted to normalized T-scores, corrected for age and gender, and centered and scaled relative to a healthy population of subjects using the MCCB scoring program {24}. The MCCB and fMRI scans were administered on the same day. Only scores from the MCCB working memory domain and the two domain subtests were used for the current analysis.

For comparison with the multicomponent model (Figure 1), the verbal subtest of MCCB working memory (Letter-Number Span) was considered to primarily test functioning of the Phonologic Loop, while the non-verbal subtest (Wechsler Memory Scale-III, Spatial Span) was considered to test the Visuospatial Sketchpad. Additionally, both working memory subtests were expected to involve the Central Executive system. However, consistent with the multicomponent model, no subtest uniquely tested this system. Instead, the Central Executive system was identified based on its association with the dlPFC and Executive Control networks. No MCCB working memory subtest was considered to adequately test the functioning of the Episodic Buffer, although a disputable association with the hippocampus has been suggested {25}.

fMRI Parameters

Images were acquired on a 3-T scanner (General Electric, Milwaukee) using a standard quadrature head coil. An inversion-recovery echo planar image (IR-EPI; TI=505 ms) was collected to improve coregistration of functional images. Functional scans were acquired with the following parameters: TR=2000 ms, TE=30 ms, field of view=240 mm^2, matrix=64×64, voxel size=3.75×3.75 mm^2, slice thickness=2.6 mm, gap=1.4 mm, interleaved, flip angle=70°. Resting fMRI scan duration was 10 minutes. Participants were instructed to rest with their eyes open.

Data Analysis

Preprocessing—MRI data were preprocessed using SPM8 (www.fil.ion.ucl.ac.uk/spm/software/spm8) for each subject individually. The first four images were excluded for saturation effects. Echo planar images from each subject were realigned to the first volume, resliced to a 3-mm^3 voxel size, and normalized to the Montreal Neurological Institute (MNI) template using unified segmentation {26}, and smoothed with an 8-mm FHWM Gaussian kernel (Figure 3, step 1).

Independent Components Analysis—Large-scale networks, or Intrinsic Connectivity Networks (ICNs), were identified using Independent Components Analysis (ICA; Figure 3, step 2). Spatial ICA was carried out on group-level data using GIFT v1.3i (http://icatb.sourceforge.net; {27}. Twenty-one components were estimated based on minimum description length (MDL) criteria and extracted using the infomax algorithm {28, 29}. Voxel time series were whitened, variance normalized, and temporally concatenated with two PCA data reduction steps, of 70 and 21 components. Spatial maps were reconstructed with GICA3 and scaled to z-scores {30}. All spatial maps and time courses were visually inspected to identify noise components. Seven components, classified as artifacts based on spatial distributions in CSF or white matter, or resulting from high-frequency oscillations, were excluded from further analysis. To identify common Intrinsic Connectivity Networks, group mean ICA spatial maps were correlated with published ICA templates {16}. Templates matching multiple ICA components were identified as subnetworks, while ICA components without template matches were classified based on anatomy. For example, two ICA components with minimal spatial overlap matched the template for the dorsal Default Mode Network (DMN). These were labeled as the anterior DMN and posterior DMN based on anatomical differences in their spatial maps (see Supplementary Materials). Another ICA component did not clearly match any template, but was strongly localized to the bilateral hippocampus and amygdala and was labeled as the bilateral medial temporal lobe network (B. MTL) based on the corresponding anatomy. Following ICA, back-reconstructed subject-specific time series for each ICN was correlated with voxels' time series in a functional connectivity analysis.

Functional Connectivity—CSF, white matter signals, and 6 movement parameters were regressed out of all time series individually for each subject. Time points with excessive movement were censored {31}. Following nuisance signal removal and movement control precautions, time series for every gray matter voxel were correlated with each ICA component time series for each subject individually (Figure 3, step 3). The resulting vector

of correlations for each voxel efficiently and comprehensively summarizes a voxel's connectivity to all networks within the brain and was used as a feature vector, after removing the influences of age, smoking status and education level using linear regression residuals {32}.

Distance Covariance Statistic—Distance covariance (dCov) is a recently developed multivariate technique that tests the statistical independence of two vectors with arbitrary dimensions {20}. The dCov statistic is zero if and only if the random vectors are independently distributed, and increasingly positive otherwise. A complete description of dCov is available in the supplementary materials, including its statistical properties, details of its calculation, an example use, and application in the current analysis.

Distance covariance analyses proceeded in two steps. First, dCov was calculated for each grey matter voxel, using subjects' connectivity vector and MCCB scores as input (Figure 3, step 4). This resulted in an unthresholded whole-brain statistical map, showing associations between voxel-level connectivity and MCCB scores in the sample. Results were then corrected for multiple comparisons using a modification of Nichol's cluster-level non-parametric test {33}. 5000 volumes were generated by permuting subject's MCCB scores for each voxel. Empirical p-values were calculated as the proportion of times the permutation dCov statistic exceeded the original dCov statistic at that voxel. Empirical p-values for all permutation voxels were calculated in an identical manner, volumes were thresholded using a cluster-defining threshold of $p<0.01$, and resulting cluster sizes calculated. A cluster was considered significant after correcting for multiple comparisons if the empirical p-value of obtaining a cluster this size or larger was significant at $p<0.05$. Significant clusters were displayed as cortical surface projections, created using Caret {34}.

Distance covariance was then applied to test connectivity using the elements of the individual vector, using an individual scalar correlation coefficient and the scalar MCCB score (Figure 3, step 5). This procedure tested the individual elements of the connectivity vector that contributed to that voxel's significance in the previous whole-brain analysis. Resulting dCov statistics for connectivity were thresholded and corrected for multiple comparisons using a cluster-level permutation procedure developed for network analysis, the Network-Based Statistic {35}. Connections were thresholded at $p<0.005$. An individual connection was considered significant after correcting for multiple comparisons if it was included in a cluster with size significant at $p<0.05$. Significant connections were displayed as two-dimensional saggital, coronal, and axial projections in MNI space, the "glass brain" format.

Results

MCCB Working Memory

All MCCB scores were corrected for age and gender, as well as centered and scaled relative to MCCB scores from a healthy population of subjects (mean of 50, with a standard deviation of 10; {24}. Subjects with schizophrenia demonstrated deficits in MCCB working memory domain (mean=43.43, sd=11.56, one-sample t-test with H_0: mu=50: $t_{27}=-3.01$, $p<0.006$). Performance on the test of verbal working memory, Letter-Number Span (LNS)

was diminished (mean=41.07, sd=12.01, one-sample t-test with H_0: mu=50: t_{27}=−3.93, p<0.006) while deficits on the test of nonverbal working memory, WMS-III Spatial Span, were less pronounced (mean=48.21, sd=10.08, one-sample t-test with H_0: mu=50: t_{27}= −0.94, p>0.10). Full results for all MCCB cognitive domains and tests are reported in the supplementary materials.

Intrinsic Connectivity Networks

Fourteen ICNs matched templates for known networks to a relatively high degree (mean r=0.38). The RECN and LECN were present, encompassing the dlPFC and vlPFC along with right or left lateralized IPS (Figure 4). The Language Network encompassed the bilateral vlPFC (including the L. IFG), TPJ, superior temporal gyri, and primary auditory cortices. An ICN consisting of bilateral medial temporal regions included the hippocampus.

Connectivity and MCCB Working Memory

Associations between working memory and connectivity were examined in a two-step procedure. First, we focused on associations to neuroanatomy, investigating where in the brain connectivity influences task performance. Next, after these regions were identified, we investigated which connections to and from the regions most contributed to task performance. This analysis both highlighted how different subregions within a larger network made different contributions to working memory, and how each region's interactions with multiple networks contributed to task performance.

Working Memory and Neuroanatomy—Voxel-level whole-brain analysis of connectivity identified associations between MCCB working memory and several regions throughout the brain (Figure 5, Table 2). These included the vlPFC bilaterally, as well as the left TPJ. Smaller clusters were located in the left hippocampus, dorsal anterior cingulate cortex, middle temporal gyrus, and the left anterior cerebellum extending into the inferior temporal gyrus. Smaller clusters in the right hemisphere were located along the right IPS, superior temporal sulcus, middle cingulate gyrus, pre-supplementary motor area, posterior hippocampus, and parietal operculum. Interestingly, dlPFC connectivity was not associated with MCCB working memory.

Working Memory and Network Connectivity—In order to better understand how connectivity to the regions in Figure 5 contributed to working memory, we then examined the individual connections of these voxels.

Many of the systems of the multi-component working memory model were significantly associated with MCCB working memory performance (Figure 6). These include the RECN and LECN for the Central Executive system, the right vlPFC and IPS for the Visuospatial Sketchpad, and the left vlPFC and TPJ for the Phonologic Loop. The small cluster within the hippocampus was not significantly connected to either the LECN or RECN (p>0.05 corrected).

In addition to connectivity predicted by the multi-component model, other networks and regions contributed to MCCB working memory. Notably, and beyond the scope of the

multicomponent model and the networks detailed above, the Default Mode Network influenced working memory through the IFG bilaterally. In contrast, Language and bilateral Medial Temporal Lobe ICNs minimally influenced working memory. See supplementary materials for full results, showing all voxels and connections significant after correcting for multiple comparisons.

Associations with Verbal and Non-verbal Working Memory

Results for the individual tests comprising the MCCB Working Memory domain were largely similar to above, with minor differences between verbal and nonverbal subtests (see supplementary materials). For the verbal LNS subtest, anatomical results were strongly lateralized to the left hemisphere and largely limited to regions within the Phonologic Loop. For the non-verbal WMS-III Spatial Span, anatomical results were bilateral and included more extensive clusters throughout the cortex. In both cases, network results mirrored the composite MCCB working memory domain.

Discussion

Overall, associations between working memory task performance and functional connectivity were in good agreement with the predictions of the hypothesis and the multicomponent model (Figures 2 & 6). A result that was not expected, however was that the dlPFC was not observed to directly influence MCCB working memory (Figure 5). Instead, dlPFC contributions to working memory were indirect, as parts of the RECN and LECN (Figure 4). While perhaps counterintuitive, these results are consistent with the concept of a distributed and delocalized Central Executive system, associated with but not limited to prefrontal regions {23, 36}. Similarly, the RECN influenced working memory through the left TPJ as well (Figure 6) even though this region was not included in this network. Alternatively, working memory tasks in the MCCB may not require processing within the dlPFC. Many previous investigations of working memory were carried out with the n-back, a relatively difficult task requiring continual updating of the information contained within working memory {12}. Tasks with low cognitive load often preferentially activate the vlPFC instead; with dlPFC active during high processing demands {10, 37}. In this view, the absence of dlPFC may reflect the low cognitive demands of MCCB tests. Lastly, these results do not contradict previous associations of the Central Executive system with the dlPFC, but instead suggest a delocalized Central Executive system that includes the dlPFC, but extends beyond any single cortical region.

The Phonologic Loop was strongly left lateralized, agreeing with the multi-component model (Figure 2). Consistent with the predictions of the model, this was especially true for the verbal LNS test with associated large clusters in the left IFG and TPJ (see supplementary materials). Interestingly, the Language Network itself was minimally associated with working memory. Based on these results, the Phonologic Loop is likely separate from the delocalized Language Network.

Regions of the Visuospatial Sketchpad, such as the right vlPFC and IPS, were present in the results, but the interpretation was not as straightforward. Processing during the nonverbal WMS-III Spatial Span subtest would be expected to rely on the Visuospatial Sketchpad.

Clusters in the right vlPFC and IPS were associated with performance on this subtest (see supplementary materials). However, these associations were bilateral, a result consistent with meta-analysis of activation during working memory fMRI tasks {10}.

It is unclear if the Episodic Buffer contributed to MCCB working memory tests. Although this system has been associated with the hippocampus, the supporting evidence is less well established {25}. In the present investigation, an association to working memory was found to a small cluster within the hippocampus (Figure 5). However, these voxels were not influenced by connections from the RECN or LECN (Figure 6). Since none of the MCCB tests involved the constructions of mental scenes from episodic long-term memory, the Episodic Buffer is unlikely to play a prominent role and a lack of any clear associations is unsurprising, if uninformative.

Previous neuroimaging investigations into working memory in schizophrenia have primarily focused on activity resulting from the n-back fMRI task. This task is notable for its robust but nonspecific activations, and its dependence on dlPFC functioning {10, 38}. In contrast, the association with the vlPFC, but not dlPFC, in Figure 5 may suggest that these tests are more likely to involve transformation of stored information and inhibition of irrelevant stimuli {10}. Alternatively, an absence of associations between dlPFC connectivity and MCCB working memory may also indicate that dlPFC dysfunction during the n-back in schizophrenia may extend these working memory tests as well {13}. Future investigations will seek to clarify this distinction, as well as to investigate the relationship between connectivity and the impact of working memory dysfunction in schizophrenia.

The current study includes several limitations. Only subjects with a diagnosis of schizophrenia or schizoaffective disorder were included. This study design was chosen because the primary aim was to investigate performance on a cognitive test designed for patients with schizophrenia and validated in this population {8}. The lack of a healthy comparison group does, however, limit study interpretation. Any extrapolation to the neurobiology of MCCB working memory in healthy subjects is premature, as results could be due to disease-specific neurobiology. The current analysis was limited to the MCCB working memory domain. Analysis of other MCCB cognitive domains and generalization of these results will be the focus of future investigations. An additional limitation is the modest sample size. Although likely adequately powered for many types of fMRI studies {39–41}, the sample size may be small for the current analysis. The risk of false positive results cannot be ruled out; however, false negatives are a greater concern in this analysis given the sample size {40}. Lastly, the validity of the central executive system itself as a concept in psychology is not without controversy {36, 42, 43}.

Conclusion

We have demonstrated that performance on the MCCB in subjects with schizophrenia can be predicted from functional connectivity, using resting state fMRI. MCCB working memory tests largely agreed with Baddeley’s multi-component model. However, the dlPFC was not directly associated with MCCB working memory. Instead, the Central Executive system was best represented by delocalized RECN and LECN. These results illuminate the complex

neurobiology underlying working memory in terms of intrinsic network architecture of the brain at rest, in an unprecedented level of detail, encompassing every voxel. Lastly, with the increasing use of MCCB in pharmaceutical development, these results can help to provide insight into the neuronal pathways and connections mediating the potential therapeutic effects of novel therapeutic strategies designed to ameliorate the cognitive symptoms of schizophrenia.

Supplementary Material

Refer to Web version on PubMed Central for supplementary material.

Acknowledgements

This work was supported by the National Institutes of Health grants R01MH102224 and R01GM117946, Veterans Administration grant I01CX000459, and by the Brain & Behavior Research Foundation.

References

1. Park S, Holzman PS: Schizophrenics show spatial working memory deficits. Arch Gen Psychiatry 1992; 49:975–82 [PubMed: 1449384]
2. Lee J, Park S: Working memory impairments in schizophrenia: a meta-analysis. J Abnorm Psychol 2005; 114:599–611 [PubMed: 16351383]
3. Silver H, Feldman P, Bilker W, et al.: Working memory deficit as a core neuropsychological dysfunction in schizophrenia. Am J Psychiatry 2003; 160:1809–16 [PubMed: 14514495]
4. Lewandowski KE, Cohen BM, Ongur D: Evolution of neuropsychological dysfunction during the course of schizophrenia and bipolar disorder. Psychol Med 2011; 41:225–41 [PubMed: 20836900]
5. Cervellione KL, Burdick KE, Cottone JG, et al.: Neurocognitive deficits in adolescents with schizophrenia: longitudinal stability and predictive utility for short-term functional outcome. J Am Acad Child Adolesc Psychiatry 2007; 46:867–78 [PubMed: 17581451]
6. Shamsi S, Lau A, Lencz T, et al.: Cognitive and symptomatic predictors of functional disability in schizophrenia. Schizophr Res 2011; 126:257–64 [PubMed: 20828991]
7. Green MF, Kern RS, Braff DL, et al.: Neurocognitive deficits and functional outcome in schizophrenia: are we measuring the “right stuff”? Schizophr Bull 2000; 26:119–36 [PubMed: 10755673]
8. Nuechterlein KH, Green MF, Kern RS, et al.: The MATRICS Consensus Cognitive Battery, part 1: test selection, reliability, and validity. Am J Psychiatry 2008; 165:203–13 [PubMed: 18172019]
9. Andrade J (ed): Working memory in perspective. Hove, East Sussex, UK, Psychology Press, 2001
10. Wager TD, Smith EE: Neuroimaging studies of working memory: a meta-analysis. Cogn Affect Behav Neurosci 2003; 3:255–74 [PubMed: 15040547]
11. Nee DE, Brown JW, Askren MK, et al.: A meta-analysis of executive components of working memory. Cereb Cortex 2013; 23:264–82 [PubMed: 22314046]
12. Owen AM, McMillan KM, Laird AR, et al.: N-back working memory paradigm: a metaanalysis of normative functional neuroimaging studies. Hum Brain Mapp 2005; 25:46–59 [PubMed: 15846822]
13. Glahn DC, Ragland JD, Abramoff A, et al.: Beyond hypofrontality: a quantitative metaanalysis of functional neuroimaging studies of working memory in schizophrenia. Hum Brain Mapp 2005; 25:60–9 [PubMed: 15846819]
14. Potkin SG, Turner JA, Brown GG, et al.: Working memory and DLPFC inefficiency in schizophrenia: the FBIRN study. Schizophr Bull 2009; 35:19–31 [PubMed: 19042912]
15. Johnson MR, Morris NA, Astur RS, et al.: A functional magnetic resonance imaging study of working memory abnormalities in schizophrenia. Biol Psychiatry 2006; 60:11–21 [PubMed: 16503328]

16. Shirer WR, Ryali S, Rykhlevskaia E, et al.: Decoding subject-driven cognitive states with whole-brain connectivity patterns. Cereb Cortex 2012; 22:158–65 [PubMed: 21616982]
17. Smith SM, Fox PT, Miller KL, et al.: Correspondence of the brain's functional architecture during activation and rest. Proc Natl Acad Sci U S A 2009; 106:13040–5 [PubMed: 19620724]
18. Bullmore E, Sporns O: The economy of brain network organization. Nat Rev Neurosci 2012; 13:336–49 [PubMed: 22498897]
19. Cole MW, Bassett DS, Power JD, et al.: Intrinsic and task-evoked network architectures of the human brain. Neuron 2014; 83:238–51 [PubMed: 24991964]
20. Szekely GJ, Rizzo ML, Bakirov NK: Measuring and testing dependence by correlation of distances. The annals of statistics 2007; 35:2769–2794
21. Baddeley AD: Working memory: looking back and looking forward. Nat Rev Neurosci 2003; 4:829–39 [PubMed: 14523382]
22. Henson R: Neural working memory. Working memory in perspective 2001; 151–173
23. Andres P: Frontal cortex as the central executive of working memory: time to revise our view. Cortex 2003; 39:871–95 [PubMed: 14584557]
24. Kern RS, Nuechterlein KH, Green MF, et al.: The MATRICS Consensus Cognitive Battery, part 2: co-norming and standardization. Am J Psychiatry 2008; 165:214–20 [PubMed: 18172018]
25. Baddeley AD, Allen RJ, Hitch GJ: Binding in visual working memory: the role of the episodic buffer. Neuropsychologia 2011; 49:1393–400 [PubMed: 21256143]
26. Ashburner J, Friston KJ: Unified segmentation. Neuroimage 2005; 26:839–51 [PubMed: 15955494]
27. Calhoun VD, Adali T, Pearlson GD, et al.: A method for making group inferences from functional MRI data using independent component analysis. Hum Brain Mapp 2001; 14:140–51 [PubMed: 11559959]
28. Bell AJ, Sejnowski TJ: An information-maximization approach to blind separation and blind deconvolution. Neural computation 1995; 7:1129–1159 [PubMed: 7584893]
29. Li YO, Adali T, Calhoun VD: Estimating the number of independent components for functional magnetic resonance imaging data. Hum Brain Mapp 2007; 28:1251–66 [PubMed: 17274023]
30. Erhardt EB, Rachakonda S, Bedrick EJ, et al.: Comparison of multi-subject ICA methods for analysis of fMRI data. Hum Brain Mapp 2011; 32:2075–95 [PubMed: 21162045]
31. Power JD, Barnes KA, Snyder AZ, et al.: Spurious but systematic correlations in functional connectivity MRI networks arise from subject motion. Neuroimage 2012; 59:2142–54 [PubMed: 22019881]
32. Hua WY, Nichols TE, Ghosh D, et al.: Multiple comparison procedures for neuroimaging genomewide association studies. Biostatistics 2015; 16:17–30 [PubMed: 24963012]
33. Nichols TE, Holmes AP: Nonparametric permutation tests for functional neuroimaging: a primer with examples. Hum Brain Mapp 2002; 15:1–25 [PubMed: 11747097]
34. Van Essen DC, Drury HA, Dickson J, et al.: An integrated software suite for surface-based analyses of cerebral cortex. J Am Med Inform Assoc 2001; 8:443–59 [PubMed: 11522765]
35. Zalesky A, Fornito A, Bullmore ET: Network-based statistic: identifying differences in brain networks. Neuroimage 2010; 53:1197–207 [PubMed: 20600983]
36. Baddeley AD: The central executive: a concept and some misconceptions. J Int Neuropsychol Soc 1998; 4:523–6 [PubMed: 9745242]
37. Smith EE, Jonides J: Working memory: a view from neuroimaging. Cogn Psychol 1997; 33:5–42 [PubMed: 9212720]
38. Barch DM, Moore H, Nee DE, et al.: CNTRICS imaging biomarkers selection: Working memory. Schizophr Bull 2012; 38:43–52 [PubMed: 22080498]
39. Desmond JE, Glover GH: Estimating sample size in functional MRI (fMRI) neuroimaging studies: statistical power analyses. J Neurosci Methods 2002; 118:115–28 [PubMed: 12204303]
40. Murphy K, Garavan H: An empirical investigation into the number of subjects required for an event-related fMRI study. Neuroimage 2004; 22:879–85 [PubMed: 15193618]
41. Mumford JA, Nichols TE: Power calculation for group fMRI studies accounting for arbitrary design and temporal autocorrelation. Neuroimage 2008; 39:261–8 [PubMed: 17919925]

42. Royall DR, Lauterbach EC, Cummings JL, et al.: Executive control function: a review of its promise and challenges for clinical research. A report from the Committee on Research of the American Neuropsychiatric Association. J Neuropsychiatry Clin Neurosci 2002; 14:377–405 [PubMed: 12426407]

43. Jurado MB, Rosselli M: The elusive nature of executive functions: a review of our current understanding. Neuropsychol Rev 2007; 17:213–33 [PubMed: 17786559]

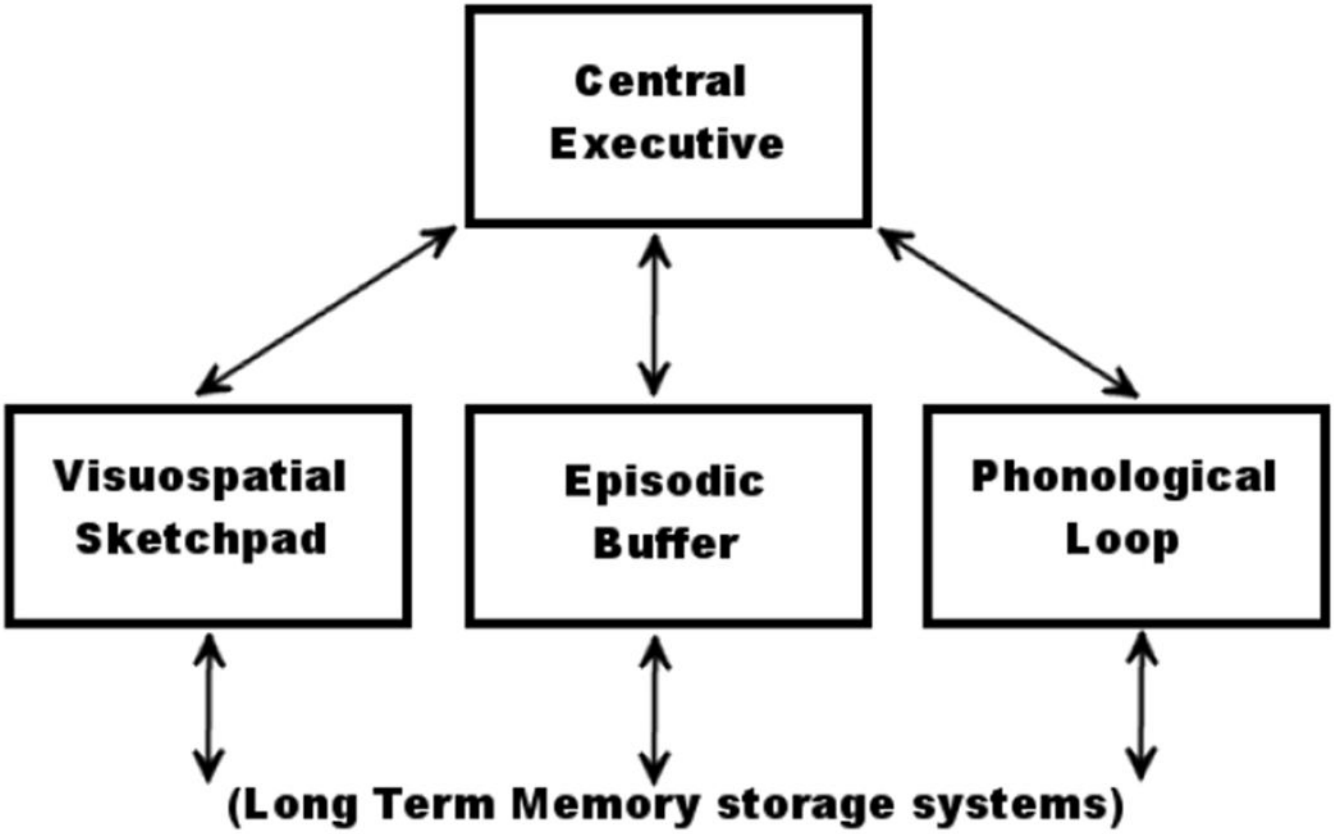

Figure 1:
Baddeley's multicomponent model of working memory. The Central Executive directs attention and is responsible for binding information from subsidiary systems into coherent episodes. Three subsidiary systems are each specialized for different types of information storage, and interact with the contents of long-term memory. The Visuospatial Sketchpad is capable of storing visual and spatial information. The Phonologic Loop is specialized for speech and linguistic information. The Episodic Buffer draws upon the contents of long-term memory to construct novel scenes in working memory.

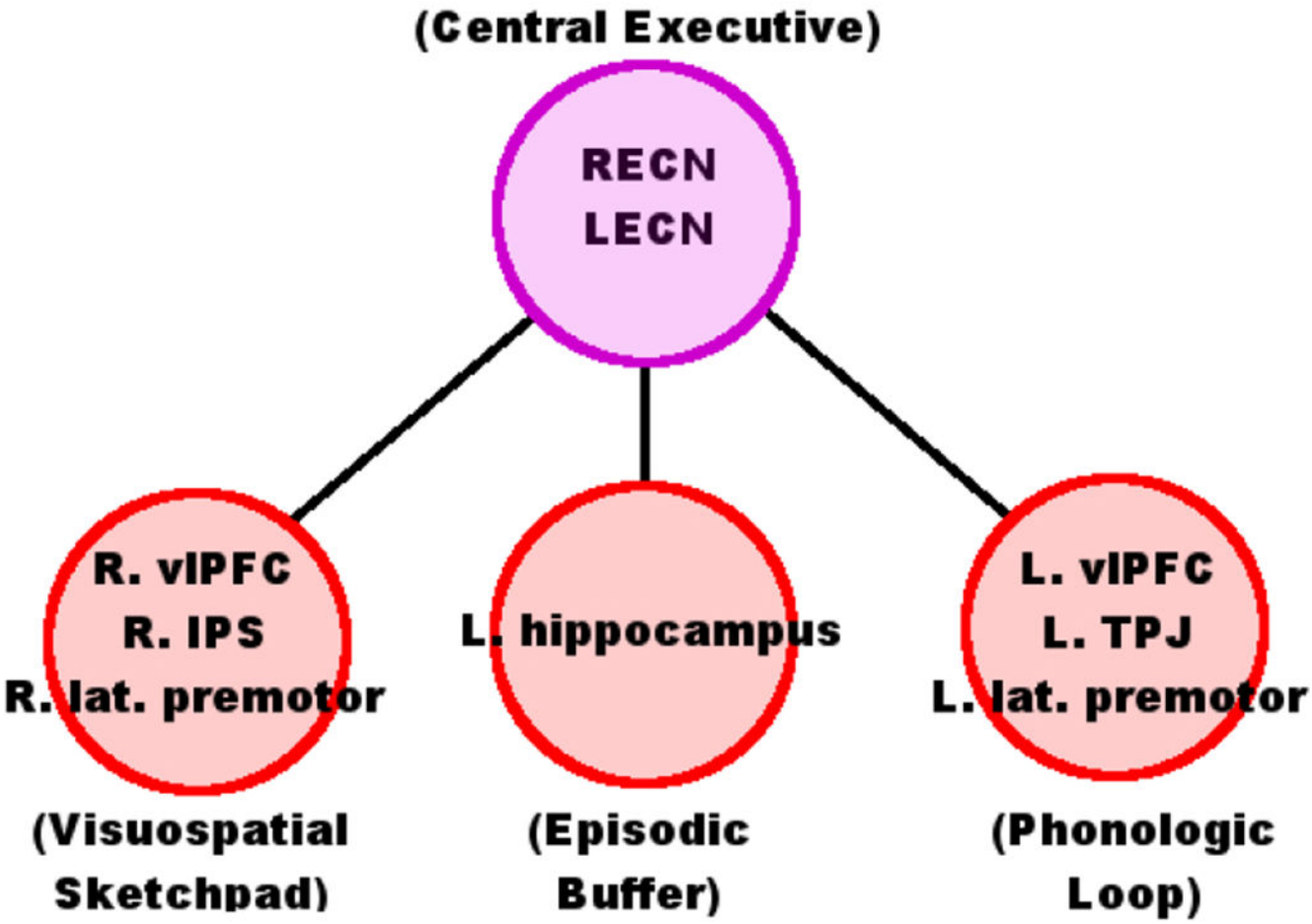

Figure 2:

Neuroanatomy of the multicomponent model of working memory. The Visuospatial Sketchpad is associated with right lateralized ventrolateral PFC (vlPFC), intraparietal sulcus (IPS), and lateral premotor cortices. The Phonologic Loop is associated with left vlPFC, temporoparietal junction (TPJ), and lateral premotor cortices. The location of the Episodic Buffer is relatively unknown, but may be associated with the left hippocampus. We hypothesize that the Central Executive will be represented by two delocalized Intrinsic Connectivity Networks, the right and left Executive Control Networks (RECN & LECN). These large-scale networks are composed of activity from many different regions, including the right and left dlPFC, but extend beyond these regions to include activity in other prefrontal and parietal areas.

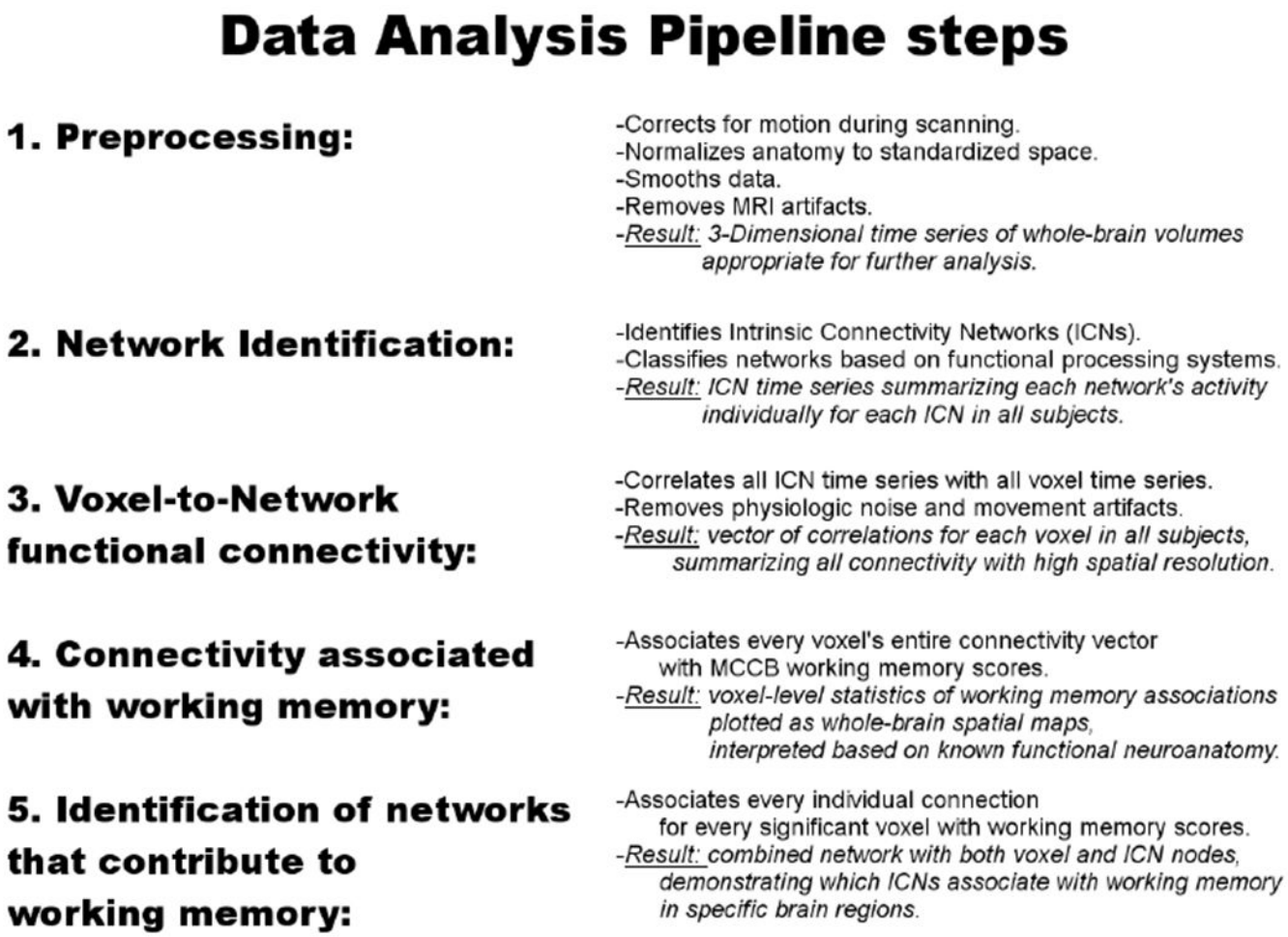

Figure 3:

Data Analysis Pipeline. 1. Data preprocessing followed standard fMRI procedures and algorithms. 2. Network Identification was carried out using Independent Components Analysis (ICA), resulting in a set of Intrinsic Connectivity Networks (ICNs). 3. Voxel-to-Network functional connectivity was carried out by correlating voxel and ICN time series. 4. & 5. Cognitive associations were investigated using Distance Covariance in two steps, first by associating each voxel's overall connectivity with working memory performance, (step 4), and subsequently to each voxel-to-network connection (step 5).

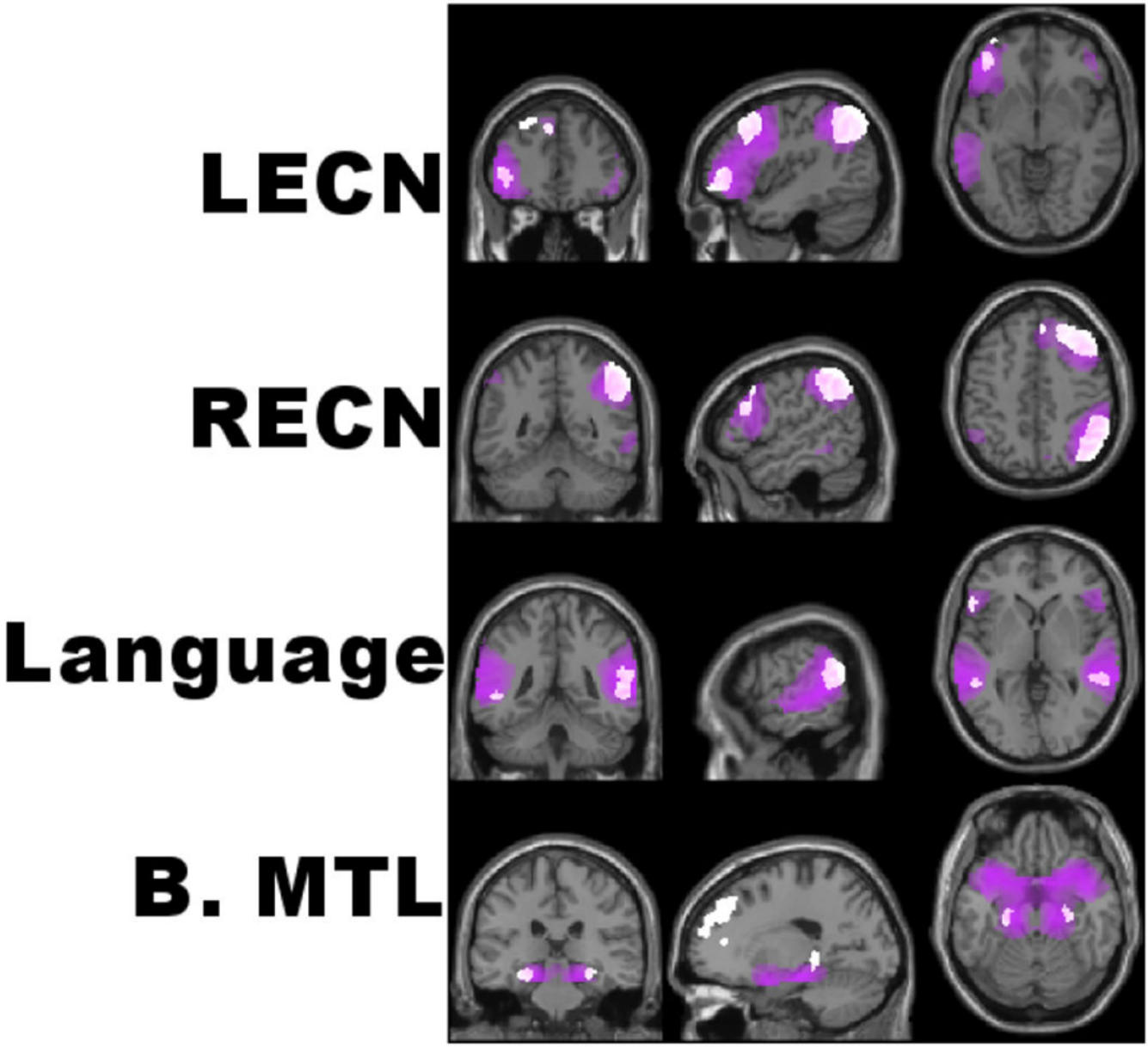

Figure 4:
Select Intrinsic Connectivity Networks (ICNs). ICNs were extracted by Independent Components Analysis, thresholded to display the top 70% of voxels (purple clusters), and overlayed with spatial maps for commonly identified templates (white clusters). Displayed are the left and right Executive Control Networks (RECN & LECN), the Language network, and an ICN encompassing the medial temporal lobes bilaterally (B. MTL). See supplementary materials for all ICNs extracted with ICA.

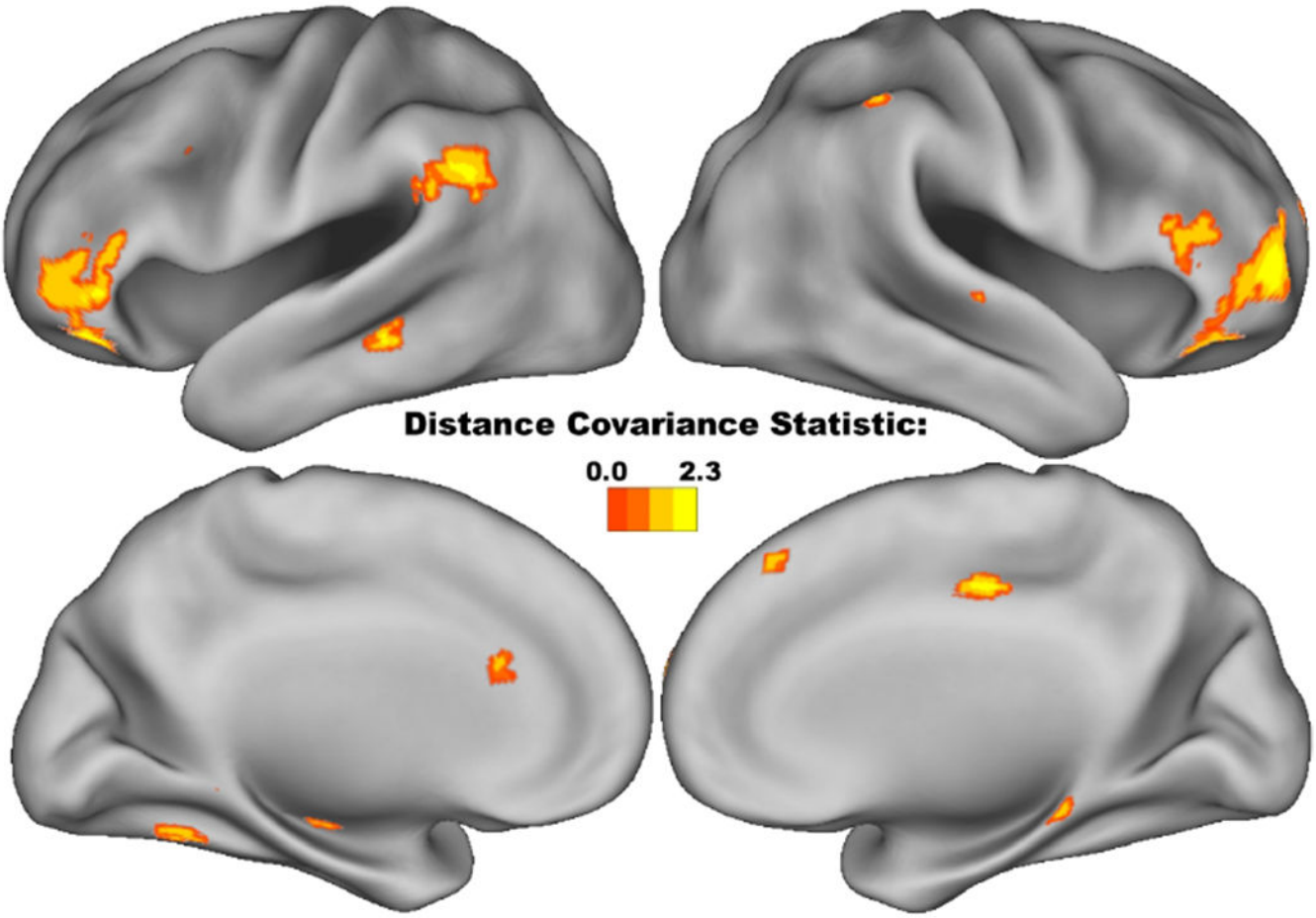

Figure 5:

Anatomical associations between voxel-level connectivity and the MCCB Working Memory domain. All voxels, with connectivity associated with MCCB working memory using Distance Covariance statistic ($p<0.05$, corrected), displayed as cortical surface renderings. Throughout the entire brain, working memory performance was most strongly associated with the bilateral vlPFC, left TPJ, and right IPS.

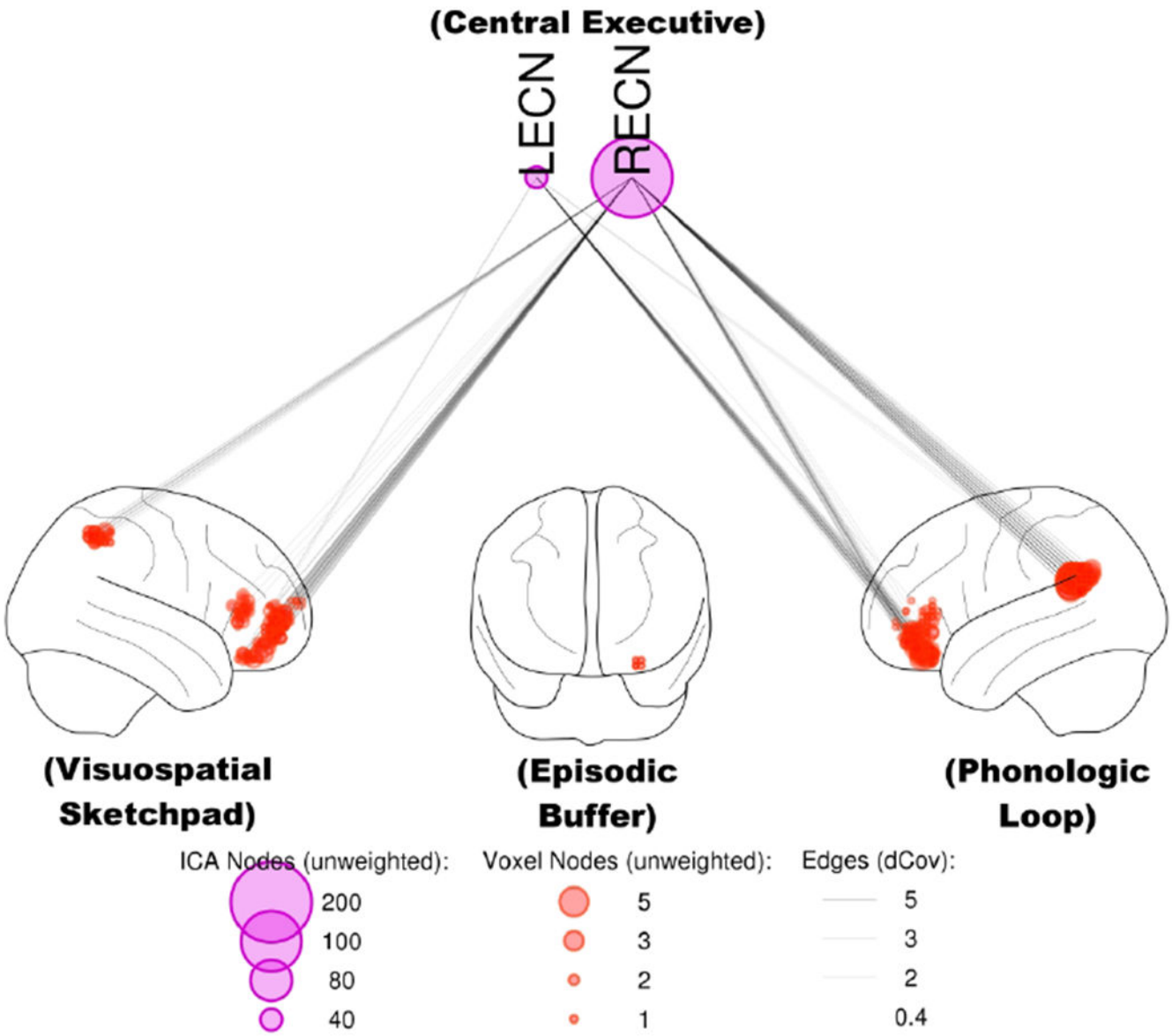

Figure 6:

Functional connectivity at rest predicts working memory test performance, in agreement with systems predicted by the multicomponent model. Connectivity between the RECN or LECN and regions within the Visuospatial Sketchpad (right vlPFC & IPS) and Phonologic Loop (left vlPFC & TPJ) was associated with MCCB working memory scores ($p<0.05$, corrected). Node size is proportional to unweighted degree (i.e., the number of significant connections, after correcting for multiple comparisons using the network-based statistic). dCov: distance covariance statistic.

TABLE 1:

Sociodemographic Information for subjects[a]

Characteristic	N	%	Mean	SD
Sex (female)	7	25.0%		
Ethnicity (AA)	5	17.9%		
Ethnicity (Hisp.)	2	7.1%		
Age (years)			42.4	12.6
Education (years)			13.4	1.81
Smoking (smokers)	14	50.0%		
Diagnosis (schizophrenia)	20	71.4%		
Diagnosis (schizoaffective)	8	28.6%		
Medications (typical antipsychotics)	7	25.0%		
Medications (atyp. antipsych.)	23	82.1%		
Medications (non-med.)	2	7.1%		
BPRS Total:			34.8	8.1
SANS Total:			4.36	2.9

[a]AA: African American, Hisp.: Hispanic; atyp. antipsych.: atypical antipsychotics, non-med.: non-medicated; BPRS: Brief Psychiatric Rating Scale; SANS: Scale for the Assesment of Negative Symptoms

TABLE 2:

Local Peak Multivariate Associations between MCCB Working Memory[a]

		MNI Coordinates:			
Region:	**Statistic (dCov):**	**x**	**y**	**z**	**Cluster Size (voxels):**
L. Supramarginal Gyrus	2.08	−51	−49	28	107
L. Angular Gyrus	1.76	−57	−55	28	
L. Supramarginal Gyrus	1.64	−45	−43	25	
L. Angular Gyrus	1.59	−48	−58	28	
L. Supramarginal Gyrus	1.52	−57	−49	22	
R. Inferior Parietal Lobule	1.91	51	−46	55	76
R. Inferior Parietal Lobule	1.73	45	−52	55	
R. Inferior Parietal Lobule	1.61	51	−52	49	
R. Inferior Parietal Lobule	1.59	45	−46	49	
R. Angular Gyrus	1.47	45	−58	49	
R. Inferior Parietal Lobule	1.43	42	−52	43	
R. Orbitofrontal Cortex	1.83	45	47	−2	122
R. Middle Frontal Gyrus	1.67	39	50	4	
R. Superior Frontal Gyrus	1.65	30	50	13	
R. Orbitofrontal Cortex	1.55	48	44	−11	
R. Middle Frontal Gyrus	1.55	39	53	13	
R. Superior Frontal Gyrus	1.46	27	56	19	
R. Superior Frontal Gyrus	1.41	21	53	13	
R. Superior Temporal Gyrus	1.78	63	−49	22	42
R. Middle Temporal Gyrus	1.55	51	−49	22	
R. Superior Temporal Gyrus	1.46	57	−43	19	
L. Orbitofrontal Cortex	1.71	−36	38	−14	32
L. Orbitofrontal Cortex	1.64	−39	44	−8	
L. Orbitofrontal Cortex	1.51	−45	41	−14	
L. Orbitofrontal Cortex	1.37	−33	29	−14	
L. Middle Temporal Gyrus	1.71	−66	−34	−11	18
L. Middle Temporal Gyrus	1.62	−63	−25	−14	
R. Middle Cingulate Cortex	1.67	6	−19	40	13
R. Superior Frontal Gyrus	1.66	27	38	46	13
L. Inferior Parietal Lobule	1.64	−36	−43	37	15
L. Precentral Gyrus	1.63	−33	11	34	22
L. Precentral Gyrus	1.46	−42	14	34	
L. Orbitofrontal Cortex	1.61	−54	32	−2	23
L. Orbitofrontal Cortex	1.44	−51	35	−11	
R. Middle Temporal Gyrus	1.6	54	−58	16	16
R. Middle Temporal Gyrus	1.59	66	−40	4	10
R. Inferior Frontal Gyrus	1.57	54	26	13	58
R. Inferior Frontal Gyrus	1.55	48	32	19	

		MNI Coordinates:			
Region:	**Statistic (dCov):**	**x**	**y**	**z**	**Cluster Size (voxels):**
R. Inferior Frontal Gyrus	1.49	45	41	28	
R. Middle Temporal Gyrus	1.55	66	−19	−8	11
L. Cuneus	1.55	0	−79	34	13
R. Angular Gyrus	1.54	54	−64	37	5
R. Medial Prefrontal Cortex	1.53	12	56	31	16
L. Cerebellar Lobule IV/V	1.52	−15	−52	−14	10
L. Fusiform Gyrus	1.45	−21	−46	−14	
R. Middle Frontal Gyrus	1.51	45	17	52	6
L. Medial Prefrontal Cortex	1.45	−6	35	40	8
L. Medial Prefrontal Cortex	1.43	3	35	43	

[a]MCCB: MATRICS Consensus Cognitive Battery; MNI: Montreal Neurological Institute, dCov: Distance Covariance